Journal of Visualized Experiments

Imaging calcium dynamics in subpopulations of mouse pancreatic islet cells

--Manuscript Draft--

Article Type:	Invited Methods Article - JoVE Produced Video
Manuscript Number:	JoVE59491R1
Full Title:	Imaging calcium dynamics in subpopulations of mouse pancreatic islet cells
Keywords:	cell signalling; confocal microscopy; pancreatic islets of Langerhans; image processing; cell heterogeneity; partial area under the curve
Corresponding Author:	Andrei Tarasov University of Oxford Oxford, Oxon UNITED KINGDOM
Corresponding Author's Institution:	University of Oxford
Corresponding Author E-Mail:	andrei.tarasov@ocdem.ox.ac.uk
Order of Authors:	Alexander Hamilton
	Elisa Vergari
	Caroline Miranda
	Andrei Tarasov
Additional Information:	
Question	**Response**
Please indicate whether this article will be Standard Access or Open Access.	Standard Access (US$2,400)
Please indicate the **city, state/province, and country** where this article will be **filmed**. Please do not use abbreviations.	Oxford, UK

OXFORD CENTRE FOR DIABETES ENDOCRINOLOGY AND METABOLISM
RADCLIFFE DEPARTMENT OF MEDICINE

Churchill Hospital, Headington, Oxford OX3 7LE
Tel: +44(0)1865 857348 Fax: +44(0)1865 857074
andrei.tarasov@ocdem.ox.ac.uk
https://www.rdm.ox.ac.uk/people/andrei-tarasov

Dr Benjamin Werth,
Senior Science Editor
JoVE

26 March 2019

Dear Benjamin,

Re: Hamilton et al revised manuscript (JoVE59491)

We thank the Journal and the Reviewers for their constructive feedback.

After over 2 months of hard work, we would like to submit the revised version of our manuscript reporting an extended protocol for microscopic imaging of real-time changes in cytosolic calcium within small subpopulations of pancreatic islet cells. We believe that we have dealt with all of the points raised by the Editors and the Reviewers, which resulted in substantial improvement of the paper.

Per the open-access query, I wonder if this option could be negotiated at a later stage.

We look forward to hearing from you in due course.

Yours sincerely,

Dr Andrei Tarasov

TITLE:

Imaging Calcium Dynamics in Subpopulations of Mouse Pancreatic Islet Cells

AUTHORS & AFFILIATIONS:

Alexander Hamilton[1,2], Elisa Vergari[1], Caroline Miranda[3], Andrei I. Tarasov[1,4,5]

[1]Oxford Centre for Diabetes, Endocrinology and Metabolism, University of Oxford. Churchill Hospital, Headington, Oxford, UK
[2]Lund University Diabetes Centre, Unit of Molecular Metabolism, Clinical Research Centre, Malmö University HospitalMalmö, Sweden
[3]Institute of Neuroscience of Physiology, Department of Physiology, Metabolic Research Unit, University of Göteborg, Göteborg, Sweden
[4]Oxford National Institute for Health Research, Biomedical Research Centre, Oxford, UK
[5]Life and Medical Sciences, University of Hertfordshire, Hatfield, United Kingdom

Alexander Hamilton (alexander.hamilton@med.lu.se)
Caroline Miranda (caroline.miranda@gu.se)
Elisa Vergari (elisa.vergari@ocdem.ox.ac.uk)

Corresponding Author:
Andrei I. Tarasov
andrei.tarasov@ocdem.ox.ac.uk

KEYWORDS:

Calcium dynamics, time-lapse imaging, islets of Langerhans, α-cells, laser scanning confocal microscopy, time series signal processing.

SUMMARY:

Here, we present a protocol for imaging and quantifying calcium dynamics in heterogeneous cell populations, such as pancreatic islet cells. Fluorescent reporters are delivered into the peripheral layer of cells within the islet, which is then immobilized and imaged, and per-cell analysis of the dynamics of fluorescence intensity is performed.

ABSTRACT:

Pancreatic islet hormones regulate blood glucose homeostasis. Changes in blood glucose induce oscillations of cytosolic calcium in pancreatic islet cells that trigger secretion of three main hormones: insulin (from β-cells), glucagon (α-cells) and somatostatin (δ-cells). β-Cells, which make up the majority of islet cells and are electrically coupled to each other, respond to the glucose stimulus as one single entity. The excitability of the minor subpopulations, α-cells and δ-cells (making up around 20% (30%) and 4% (10%) of the total rodent[1] (human[2]) islet cell numbers, respectively) is less predictable and is therefore of special interest.

Calcium sensors are delivered into the peripheral layer of cells within the isolated islet. The islet or a group of islets is then immobilized and imaged using a fluorescence microscope. The choice

of the imaging mode is between higher throughput (wide-field) and better spatial resolution (confocal). Conventionally, laser scanning confocal microscopy is used for imaging tissue, as it provides the best separation of the signal between the neighboring cells. A wide-field system can be utilized too, if the contaminating signal from the dominating population of β-cells is minimized.

Once calcium dynamics in response to specific stimuli have been recorded, data are expressed in numerical form as fluorescence intensity vs. time, normalized to the initial fluorescence and baseline-corrected, to remove the effects linked to bleaching of the fluorophore. Changes in the spike frequency or partial area under the curve (pAUC) are computed vs. time, to quantify the observed effects. pAUC is more sensitive and quite robust whereas spiking frequency provides more information on the mechanism of calcium increase.

Minor cell subpopulations can be identified using functional responses to marker compounds, such as adrenaline and ghrelin, that induce changes in cytosolic calcium in a specific populations of islet cells.

INTRODUCTION:

The purpose of the method is to image real-time changes in cytosolic calcium concentration ($[Ca^{2+}]_{cyt}$) in minor subpopulations of pancreatic islet cells. This allows uncovering the mechanisms governing hormone secretion in these cells, revealing details about the cross-talk between different cell types and, potentially, introducing a populational dimension into the larger picture of islet signaling.

Islets consist of several cell types. Besides the more well-known insulin-secreting β-cells, there are at least two subpopulations that are also critical in regulating blood glucose[3]. α-Cells (that make up around 17% of islet cells) secrete glucagon when blood glucose gets too low, which signals for release of glucose into the bloodstream from depots in the liver. Excessive glucagon levels (hyperglucagonemia) and impaired control of glucagon-release accompany (and, technically, can contribute to) the prediabetic condition of impaired insulin sensitivity[4]. δ-Cells (around 2%) secrete somatostatin in response to glucose elevation. This ubiquitous peptide hormone is likely to be present at high concentrations in the vicinity of α- and β-cells within islets, which has a strong G_i receptor-mediated attenuating effect on both glucagon and insulin secretion.

α-Cells and δ-cells share a large part of the glucose-sensing machinery with their close lineage relatives, β-cells. All three cells types are equipped with ATP-sensitive K^+ channels, elaborate metabolic sensors[5] that control the plasma membrane potential of these excitable cells. At the same time, secretion of insulin, somatostatin and glucagon is regulated differently by glucose. Imaging of Ca^{2+} dynamics in the two minor subpopulations of islet cells can therefore provide an insight into the cross-talk between blood glucose and islet secretory output.

Early attempts of monitoring the excitability of α- and δ-cells using patch-clamp electrophysiology were soon followed by imaging of Ca^{2+} in single α- and δ-cells. The identity of

cells in these experiments was verified via a posteriori staining with anti-glucagon or anti-somatostatin antibodies. These efforts were frequently hampered by the finding that islet cells behave very differently within the islet and as single cells. Although β-cells may appear to be the main benefactors of the islet arrangement (due to their overwhelming majority that underlies their strong electrical coupling), the main discrepancy was, surprisingly, found in α-cells. Within the intact islet, these cells are constantly and persistently activated at low glucose, which is only true for around 7% of single dispersed α-cells[6]. Reporting the activity of α- and δ-cells within intact islets is therefore believed to represent a closer approximation of in vivo conditions.

In general, there are two ways of reporting Ca^{2+} dynamics specifically from the α-cell or δ-cell subpopulations: (i) expressing a genetically encoded Ca^{2+} sensor via a tissue-specific promoter or (ii) using marker compounds. The more elegant former approach adds the substantial advantage of true 3D imaging and hence studying of cell distribution within the islet. It cannot however be applied for intact human islet material. Another potential concern is the 'leakiness' of the promoter, particularly when the β-/α-cell transdifferentiation or α-cell response to high glucose is in place. The latter approach can be used with freshly isolated tissue including human samples or cultured islets. The data, however, is collected solely from the peripheral layer of islet cells, as delivering the dye/marker molecule in deeper layers without altering the islet architecture is challenging. An unexpected advantage of the latter approach is the compatibility with wide-field imaging mode, which allows scaling up the experiments to simultaneous imaging of tens or hundreds of islets (i.e., thousands to tens of thousands of cells).

Calcium is imaged in vivo using genetically encoded GCaMP[7] (or pericam[8]) family sensors, which are variants of circularly permutated green fluorescent protein (GFP) fused to the calcium-binding protein calmodulin and its target sequence, M13 fragment of myosin light chain kinase[7,9]. GCaMPs have superb signal-to-noise ratios in the range of nanomolar Ca^{2+} concentrations and a high 2-photon cross-section, which makes them an ideal choice for in vivo work[10,11]. The challenging aspect of using recombinant sensors is their delivery into the cells. Heterologous expression requires using a viral vector and multi-hour ex vivo culturing, which frequently raises concerns regarding potential de-differentiation or deterioration of cell functions. Although mouse models pre-engineered to express GCaMP address this problem, they add new challenges by increasing the lead time substantially and limiting the work to a non-human model. Very high sensitivity to changes of intracellular pH is another adverse side of protein-based sensors[12], which is, however, less of a problem for sensing oscillatory signals, such as Ca^{2+}.

The advantage of trappable dyes (such as green fluorescent Fluo4) is that they can be loaded into freshly isolated tissue within around an hour. Predictably, trappable dyes have lower signal-to-noise ratios and (much) lower photostability than their recombinant counterparts. We cannot confirm[13] the reports of toxicity of the trappable dyes[14], however, dye overloading is a frequent problem.

Red recombinant Ca^{2+} sensors based on circular permutation have been evolving rapidly since 2011[15], and most recent developments present a strong competition to GCaMPs[16] for tissue imaging, given higher depth of penetration of red light. Commercially available red trappable

dyes can be used reliably for single-cell imaging but, on the tissue level, cannot compete well with the green analogs.

There is seemingly very little choice of imaging technology for experiments in tissue where out-of-focus light becomes a critical problem. The confocal system provides acceptable single-cell resolution by cancellation of the out-of-focus light with any objective on the NA above 0.3 (for the case of GCaMP6) or 0.8 (trappable dye). In a technical sense, a conventional confocal microscope can be used for simultaneous imaging of $[Ca^{2+}]_{cyt}$ from hundreds (GCaMP) or tens of islets (trappable dye). The only realistic alternative to confocal mode in case of 3D expression of the sensor in tissue is perhaps light-sheet microscopy.

Things are slightly different for the case when the sensor is expressed in the peripheral layer of cells within the islet tissue. For bright recombinant sensors that have a vivid intracellular expression pattern, using a wide-field imaging mode with a low-NA objective may provide sufficient quality and reward the researcher with a substantial increase in the field of view area and hence the throughput. A wide-field system provides poorer spatial resolution, as the out-of-focus light is not cancelled; therefore, imaging tissue with high-NA (low depth of field) objectives is less informative, as the single-cell signal is vastly contaminated by neighboring cells. The contamination is much smaller for low-NA (high depth of field) objectives.

There are tasks, however, for which high throughput and/or sampling rate become a critical advantage. α- and δ-cells exhibit substantial heterogeneity, which creates a demand for high sample sizes to reveal the contribution of the subpopulations. Wide-field imaging is fast and more sensitive, with an industrial-scale large field-of-view system imaging hundreds (GCaMP) or tens (Fluo4) of islets at the same signal-to-noise ratio as the confocal experiments on ten or a single islet, respectively. This difference in throughput makes the wide-field system advantageous for populational imaging with a single-cell resolution, which can be especially critical for small subpopulations such as the δ-cell one. Likewise, attempts to reconstruct electrical activity from Ca^{2+} spiking[17] would benefit from the higher sampling rate provided by a wide-field imaging mode. At the same time, several “niche” problems like the activity of pancreatic α-cells upon stimulation of the dominating β-cell subpopulation, require the use of a confocal system. A factor that influences the decision towards confocal mode is the presence of substantial contaminating signal from the β-cell subpopulation.

Although using hormone-specific antibody staining to verify the identity of the cells after the imaging experiments is still an option, minor cell subpopulations can be identified using functional marker compounds, such as adrenaline and ghrelin that were shown to selectively stimulate Ca^{2+} dynamics in α-[18] and δ-cells[19,20], respectively.

The analysis of time-lapse imaging data aims to provide information beyond trivial pharmacology, such as populational heterogeneity, correlation and interaction of different signals. Conventionally, imaging data is analyzed as intensity vs. time and normalized to the initial fluorescence (F/F_0). Baseline correction is frequently needed, due to the bleaching of the fluorophore signal or contamination by changes in autofluorescence or pH (typically induced by

millimolar levels of glucose[12]). Ca^{2+} data can be analyzed in many different ways, but three main trends are to measure changes in the spike frequency, the plateau fraction, or area under the curve, computed vs. time. We found the latter approach advantageous, especially in application to heavily undersampled confocal data. The advantage of the pAUC metric is its sensitivity to both changes in signal frequency and amplitude, whereas computing the frequency requires a substantial number of oscillations[21], which is hard to attain using conventional imaging. The limiting factor of pAUC analysis is its high sensitivity to baseline changes.

PROTOCOL:

All methods described here were developed in accordance with the United Kingdom Animals (Scientific Procedures) Act (1986) and the University of Oxford ethical guidelines.

1. Isolate mouse pancreatic islets

1.1. Prepare the culture medium and the isolation solution.

1.1.1. Make up the culture medium: RMPI1640 (see **Table of Materials**), supplemented with 10% of fetal calf serum, 100 units/mL penicillin, 100 µg/mL streptomycin. Dispense the medium into two 60 mm plastic Petri dishes (not treated with any adhesive), and keep the dishes in the incubator (37 °C, 5% CO_2, absolute humidity).

1.1.2. Make up the isolation solution (50 mL/mouse): Hanks' medium with 5 mM glucose, 100 units/mL penicillin 100 µg/mL streptomycin. Keep on ice (4 °C).

1.1.3. Make up the enzyme solution (e.g., Liberase): 0.2 mg/mL in the isolation solution, 2 mL per mouse. Keep on ice (4 °C). Optionally, pre-test the activity of liberase, and optimize the incubation parameters for each batch of the enzyme[22].

1.2. Inject the enzyme solution into the mouse bile duct.

1.2.1. Sacrifice the mouse (12-week old female, C57Bl/6J) via cervical dislocation.

1.2.2. Under a dissection microscope, cut open the skin and muscle layers using fine scissors and locate the bile duct.

1.2.3. Ligate the intestine on both sides of the junction with the bile duct, using a cotton thread.

1.2.4. Lift the bile duct gently with curved fine watchmaker's forceps and introduce the ice-cold enzyme solution into the duct using a 2 mL syringe with a 30G needle. An inflation of the pancreas should be observed at this stage.

1.2.5. Collect the inflated pancreas using a combination of blunt-nosed thumb forceps and fine watchmaker's forceps into a 15 mL falcon tube and keep it on ice (4 °C). Add 1 mL of the enzyme

solution into the tube.

1.3. Liberate and collect the pancreatic Islets from the pancreas.

1.3.1. Incubate the pancreata inflated with the enzyme solution for 16 min in a water bath, at 37 °C. Gentle shaking can be used but is not critical, provided the inflation has been good.

1.3.2. Stop the digestion by addition of ice-cold isolation solution, up to 10 mL. Gently shake the digest: it should fall into small pieces.

1.3.3. Wash the digest three times in 10 mL of the isolation solution, let stand 5 min at 1 x *g* to sediment the liberated islets, on ice. Aspirate the supernatant gently, with a 10 mL serological pipette.

1.3.4. Add cold RPMI to the digest (to make up to 10 mL).

1.3.5. Use plastic Petri dishes (step 1.1.1) to pick the islets. Decant the RMPI medium off one of the Petri dishes, and gently pour some (4-5 mL) of the digest instead. Collect the liberated islets that appear as round, smooth and high-density pieces, with a P10 pipette into the second Petri dish.

1.3.6. Culture the islets in the incubator (37 °C, 5% CO_2, absolute humidity). The experiment can be paused at this stage. Leaving the islets for 1-2 hours is believed by some to help to recover from the mechanical stress during the isolation.

2. Load the dye or express the sensor

2.1. Prepare the trappable dye.

2.1.1. Dissolve the aliquot (normally, 50 µg) of the trappable dye (e.g., Fluo-4) in DMSO to a stock concentration of 2 mM. Add pluronic acid to a final concentration of 1% (using a 20% stock in DMSO), to improve the solubilization of the dye.

2.1.2. Aliquot the dye in small PCR tubes (2 µL into each). The dye can be stored frozen (-20 °C) for several weeks.

2.2. Alternatively, prepare the recombinant sensor.

2.2.1. Distribute the sensor (e.g. adenoviral vector encoding GCaMP6f) into 10 µL aliquots and store at -80 °C.

2.2.2. (Optionally) pre-test the titer of the viral stock by infecting islets (as below) using several serial dilutions, to reveal the optimal concentration for infection.

NOTE: Recombinant sensors encoded by different vectors (lentivirus, BacMam, AAV) require a different infection protocol. Make sure to check this with the vector provider and optimize the working ratio for your needs. The “working” stock of the adenovirus can be stored at -20 °C and frozen/thawed several times. Excessive freeze-thaw cycling reduces the effective titer of the virus.

2.3. Prepare the imaging solution.

2.3.1. Make up the imaging solution, mM: 140 NaCl, 4.6 KCl, 2.6 $CaCl_2$, 1.2 $MgCl_2$, 1 NaH_2PO_4, 5 $NaHCO_3$, 10 HEPES (pH 7.4, with NaOH).

2.3.2. Make up a stock of glucose (0.5 M) and mannitol (0.5 M) in the imaging solution. The stock can be stored in the fridge (4 °C) for several weeks.

2.4. Load the trappable dye.

2.4.1. Make up the dye working solution by dissolving 2 µL of the dye in 600 µL of the imaging solution containing 6 mM glucose. The solution can be heated up or vortexed to improve the solubilization.

2.4.2. Load the islets isolated in step 1 into the working solution of the dye. The loading can be done using a multiwell plate or a Petri dish. In the latter case, place a 100 µL droplet of the working solution on the bottom of a non-adhesive Petri dish (35- or 60-mm) and pipette 10-30 islets into the droplet.

2.4.3. In case of different groups of islets (e.g. wild-type/knock-out), arrange multiple wells and multiple droplets so the loading can be done simultaneously.

2.4.4. Incubate the islets in the dye working solution at room temperature in the darkness for 70-90 minutes. Do not over-incubate.

2.4.5. Check the loading under the fluorescence microscope; the islets should gain mild fluorescence, with some cells being brighter than the rest. Rounding up of cells and nuclear localization of the dye are signs of overloading.

2.4.6. Transfer the islets into dye-free imaging solution containing 6 mM glucose. The islets can be used for imaging immediately, but optionally the dye can be left to de-esterify for another 10-15 minutes. Islets will retain the dye for several hours and therefore can be used for imaging in several shifts.

2.5. Alternatively, infect the islets with the recombinant vector.

2.5.1. Plate the islets in droplets in RPMI culturing medium (step 1.1.1) (e.g., 30 µL), to minimize the volume of vector needed.

2.5.2. Add the vector at a ratio of approximately 10^5 infectious units/islet that should ideally result in multiplicity of infection >2. Ideally the ratio should be optimized to the minimal ratio that would provide expression in the peripheral layer. Pre-titration (step 2.2.2) may help.

2.5.3. Introduce 20-50 islets into the droplet and culture for 8-48 hours. (Ideally, overnight). Islets should develop a faint green fluorescence in most of the cells, without changes in cell morphology.

NOTE: The success of the infection and expression depends on the time of exposure to the virus solution. Ideally, the virus should stay in the solution overnight but can be optionally removed after as little as 15 minutes. However, infectivity, and therefore expression, is likely to be dramatically lower.

3. Imaging Ca^{2+} dynamics

3.1. Immobilize the islets under the (inverted) microscope.

3.1.1. Assemble the imaging chamber for inverted microscopy. Position the glass coverslip (thickness 1 or 1.5) inside the chamber and make sure that the glass-chamber interface is water-tight. Check that the coverslip is within the reach of the microscope objective (critical for the case of a bulky high-NA objective).

3.1.2. Prepare the immobilization accessories. Cut small rectangles (20 mm x 20 mm) from the fine mesh and the coarse mesh. Introduce two spacer "walls" on the fine mesh using a 45-50 µm thick sticky tape. Use double layers of the spacer if the size of the islets to-be-imaged substantially exceeds the conventional 100 µm.

3.1.3. Immerse the meshes and the weight into the imaging solution using a 35 mm Petri dish. Make sure that the plastic and the metal are wet.

3.1.4. Under a dissection microscope, turn the fine mesh with the spacer "walls" upside down, the spacers facing upwards. Pick several islets loaded with the trappable dye or expressing the recombinant sensor with a P20 pipette and gently position them on top of the fine mesh, between the two spacers. Ensure that the mesh and the washers do not contain excessive amounts of the imaging solution on them.

3.1.5. Pick up the mesh with the islets, using watchmaker's forceps, and position it upside down inside the imaging chamber, so that the spacers face downwards and sit directly on the chamber coverslip. Ensure that the islets are trapped between the spacers and the mesh, in the middle of the coverslip.

3.1.6. Position the coarse mesh and the weight on top of the fine mesh within the chamber. Introduce the imaging solution into the chamber. Ensure that the islets are immobilized and

ready to be imaged. Avoid excessive shaking of the chamber (small perturbations like carrying the chamber to the microscope and inserting into a heated stage are acceptable).

NOTE: A similar immobilization arrangement can be applied for an upright system.

3.2. Set up the microscope.

3.2.1. Choose the imaging mode and the objective, position the chamber with the islets from step 3.1 on the temperature-controlled stage of the microscope.

3.2.1.1. Set the temperature control (ideally, between 30 °C and 36 °C) and the perifusion. For an inverted system, position the inflow lower than the outflow within the chamber, and set the outflow flux to be greater than that of the inflow (which is typically achieved by using a tubing of a wider inner diameter on a peristaltic pump).

3.2.1.2. Ensure that the outflow has a minimal contact surface with the solution, so that it removes the solution in multiple sequential small droplets, avoiding long intervals of continuous solution removal. The latter is the major source of artefact in time-lapse imaging of the periodical signals as they appear as regular periodic intensity oscillations of every imaged pixel and are frequently interpreted as “slow waves”.

3.2.1.3. Initiate the perifusion with the imaging solution containing 3 mM glucose.

3.2.2. Choose the light path and filters for imaging of the green fluorophores; excitation between 470 and 500 and emission between 505 and 550 would work for each of them.

3.2.3. Run live imaging to set up the imaging parameters. Adjust the view to capture the islets of interest.

3.2.4. Optimize the signal-to-noise ratio of the image. To that end, adjust the excitation light intensity, the exposure time and the binning. Ensure that the settings allow a distinct visualization of each cell within the islet at the minimal possible light intensity and exposure.

3.2.5. Perform image acquisition. Depending on the task, images can be taken at 0.1 to 5 Hz. This is well below the Nyquist criteria for the fast Na^+-driven oscillations in α- and δ-cells (>300 Hz), which means that the data is undersampled by default. However, increasing the acquisition frequency to match this demand is not feasible in multicellular/multi-islet imaging with a large field of view. GCaMP can be imaged faster, whereas Fluo4 will inevitable bleach under fast acquisition conditions.

NOTE: Given that $[Ca^{2+}]_{cyt}$ oscillations in the islet cells are driven by electrical activity, using low acquisition rates may sound counterproductive. In reality, however, acquisition rates at around or above 1 Hz may be sufficient for resolving β-cell spiking behavior[13], whereas the threshold for detection of sodium channel-driven oscillations in α- and δ-cells is well above 300 Hz. Whether

the α- or δ-cell $[Ca^{2+}]_{cyt}$ oscillations are acquired at 1 Hz or 0.1 Hz, they will be severely undersampled and reflect Ca^{2+} handling by the cell rather than electrical activity.

3.2.5.1. Check the quality of the acquired data: at 3 mM glucose, α-cell activity should be clearly visible/detectable. Ensure this is the case and proceed to full-scale time-lapse imaging.

3.3. Time-lapse imaging

3.3.1. Make use of an online chart of the signal dynamics, implemented in the acquisition software if this is available. If online charting is not an option, apply a look-up-table that displays the signal intensity in the most comprehensive way (such as "rainbow").

3.3.2. Apply the stimuli in a reversible manner: record the recovery of the signal to the basal level. Ignore the artefacts at the very start and the end of the recording; the latter may look like irreversible "increase"/"decrease" of the probe fluorescence due to changes in pH or cell death.

3.3.3. Differentiate α-cells by oscillatory Ca^{2+} dynamics, at low glucose. Introduce adrenaline or glutamate into the bath solution, reversibly for 2-5 min. A rapid jump in $[Ca^{2+}]_{cyt}$ followed by a slow-down or cancellation of the oscillations will follow.

NOTE: Adrenaline is a recognized marker compound for α-cells, that has a selective positive effect on this subpopulation of islet cells, mediated by the release of Ca^{2+} from intracellular depots[18]. Glutamate has been put forth as another α-cell specific agonist[23].

3.3.4. Add/remove ghrelin, which has been recently reported to activate δ-cell selectively[19,20]. Observe a rapid reversible increase in $[Ca^{2+}]_{cyt}$ in a small subpopulation of islet cells.

3.3.5. Add/remove 20 mM glucose. Observe a coordinated oscillatory response in the β-cell subpopulation. Note the response of cells that have earlier been activated by adrenaline or glutamate and ghrelin.

3.3.6. Save the image sequence. Consider using "AutoSave" during the recording.

4. Analyzing the data

4.1. Analyze the time-lapse image.

4.1.1. Import the time-lapse image into an image analysis software, such as an open-source ImageJ/FIJI.

4.1.2. If substantial/rapid movement has occurred during the recording, discard the data as unrepairable. Use StackReg or TurboReg plugins[24] to correct minor drifts.

4.1.3. Create a mask image for cell detection and region of interest (ROI) mapping. The preferred

way to achieve this would be to make a stack image using one of the functions such as “average intensity” or “maximal intensity”. The function to be used is the one that will provide the best recognition of individual cells.

4.1.4. Threshold the mask image, remove all the data outside the islet region. The function works in automatic mode for 32-bit images.

4.1.5. Detect maxima in the threshold image. The maxima can be represented by points, regions or even sectors, if the image is dense.

4.1.6. Apply the “find maxima” function without any size restrictions and paste the detected maxima into the region of interest (ROI) editor.

4.1.7. Smooth/interpolate each of the ROIs mapped; possibly, the ROIs will require expansion. A simple script can be written for (4.1.5-4.1.7) and run several times to provide best cell detection results. Several ROIs may overlap but this is rare.

4.1.8. Analyze the position of the ROIs and paste the respective X and Y data into the electronic table software (e.g., Microsoft Excel).

4.1.9. Analyze the grey intensity vs. time for all the ROIs and paste the data into the electronic table software.

4.2. Analyze the numerical data.

4.2.1. Import the data into the data analysis software. Depending on the choice of the software and the duration/sampling/size of the experiment, this can be a simple copy-paste operation or a standalone procedure. Ensure the arrangement and storage of the numerical data.

4.2.2. Import the time-stamps or the time notes, if available.

4.2.3. Normalize the raw fluorescence intensity data (“F”) to the initial value of fluorescence (“F_0”). This does not need to be the fluorescence in the very first point but could be the average of several first points. The normalization should reduce the variability of the data and, in an ideal case (no drifting baseline) result in an analyzable dataset (“F/F_0”).

4.2.4. If the cell-to-cell variability of the F/F_0 dataset is still substantial (long recording, bleaching), perform the baseline correction. To that end, define a ‘control’ region, i.e. the range of time during which the control solution (for mouse pancreatic islets, 3 mM glucose without any agonists/antagonists) was applied.

4.2.4.1. If the control region has a clear non-oscillatory signal, assume that F/F_0 was returning to the initial value ($F/F_0=1$) after each application of the control solution. Correct the time-lapse data for each cell by splitting the data into segments, separated by the points when

485 the control solution was added, and applying linear correction to each segment. Do not use
486 polynomial or other nonlinear correction as this results in artefacts.
487
488 4.2.4.2. If the control range has clear oscillations or additional factors (such as FAD
489 autofluorescence) are present, use a spike detection algorithm[17]. A trivial and fast run-around for
490 that is a maxima-sensitive wavelet transform (**Figure 3A**).
491
492 4.2.5. Quantify the data. Although Ca^{2+} is a highly dynamic signal, presenting the Ca^{2+} data in
493 terms of absolute F/F_0 values is widely acceptable in biomedical literature. If the results from
494 multiple experiments need to be compared, choose a metric.
495
496 4.2.5.1. Measure the frequency of Ca^{2+} spikes (**Figure 4A,D**), and its response to addition
497 of (ant)agonists. To that end, split the recording into equal time intervals and compute the
498 timecourse of the partial frequency (spiking frequency in each of the intervals) by counting spikes
499 within the interval and normalizing to the interval duration.
500
501 4.2.5.2. Alternatively, set the threshold and compute the plateau fraction (pf) for each of
502 the intervals defined above (**Figure 4B,F**). The fraction indicates the percentage of time within
503 the interval that the cell spent in the "excited" state.
504
505 4.2.5.3. Alternatively, compute the partial area under the curve (pAUC) for each of the
506 intervals defined above (**Figure 4C,G**). This metric is sensitive to changes in both frequency and
507 amplitude of spiking.
508
509 NOTE: One caveat for measuring frequency is its lack of sensitivity for the spike duration and poor
510 stability. As the data is heavily undersampled vs. the electrical spiking, the number of spikes per
511 interval is quite small and hence a sole extra spike can dramatically affect the result. The
512 'bottleneck' of the pAUC is its sensitivity to changes in the baseline. Although less prone to
513 artefacts and more sensitive to changes in $[Ca^{2+}]_{cyt}$ than frequency, pAUC nevertheless is not very
514 informative about the nature of Ca^{2+} dynamics. Plateau fraction is an expansion of the open
515 probability concept to the whole-cell system. It is less robust than pAUC though, due to its
516 dependence on the threshold value.
517
518 **REPRESENTATIVE RESULTS:**
519 Islets load fairly well with the trappable dyes (**Figure 1A**), unless the lipid composition of the
520 membrane has been affected (e.g., by chronic exposure to fatty acids). The human adenovirus
521 type 5 (Ad5) vector also targets all islet cells (**Figure 1B**). Problems may arise when more than
522 one recombinant sensor is being expressed in the same cell. Furthermore, islets are typically very
523 well immobilized using the technology described above, which provides exceptional stability and
524 solution access.
525
526 Ca^{2+} spiking in α-cells can be readily detected at low glucose levels (**Figure 2**). There is a high cell-
527 by-cell correlation between the activity at low glucose and the response to adrenaline and
528 glutamate. Ghrelin activates some adrenaline-responsive cells (α-cells?) at low glucose yet it has

no effect on Ca^{2+} dynamics in most of the cells that are activated by low glucose (β-cells).

When analyzed in terms of partial frequency (**Figure 4A,C**), adrenaline- or ghrelin-stimulated cells display a substantial increase under the all-or-nothing conditions. That is, a cell with low basal activity that gets activated by adrenaline or ghrelin exhibits a dramatic increase in this metric. However, the overall changes between basal spiking and the adrenaline effect are very subtle (**Figure 4A,C**). In contrast, partial AUC is sensitive to the changes introduced by adrenaline in all cells, even when basal activity is high (**Figure 4B,D**).

FIGURE AND TABLE LEGENDS:

Figure 1: Loading of the trappable dye and expression of the recombinant sensor in islets.
Typical mouse islets loaded with the trappable dye Fluo-4 (**A**) or expressing the recombinant sensor GCaMP6 in the peripheral layer of cells (**B**) or in the deeper layer (**C**). Polar tracer sulforhodamine B (SRB, shown as white) has been utilized to outline individual cells within each islet[25]. (**D**) Representative kinetics of Ca^{2+} in response to glucose recorded from individual cells within the islet using Fluo4. Note the heterogeneity within minor cell populations.

Figure 2: Typical Ca^{2+} response of islet cells to various stimuli.
Typical α-cell (**A**) and δ-cell (**B**) Ca^{2+} dynamics, in response to adrenaline, glutamate, ghrelin, glucose. (**C**)-(**D**) Heat maps of the islet cell response showing adrenaline-positive (**C**) and ghrelin-positive (**D**) subpopulations.

Figure 3: Baseline correction.
Baseline correction

Figure 4: Analysis of the time-lapse data.
Analysis of the Ca^{2+} dynamics in α-cells. Partial frequency (**A**), plateau fraction (**B**) and area under the curve (**C**) of an α-cells $[Ca^{2+}]_i$ trace. Populational $[Ca^{2+}]_i$ data from a mouse pancreatic islet expressed as raw (F/F_0) (**D**), partial frequency (**E**), plateau fraction (F) and area under the curve (**G**).

DISCUSSION:
There are three stages in the protocol that are critical for overall success. Successful injection of the Liberase enzyme into the bile duct determines not just the quantitative success of the isolation procedure but also impacts the quality of the isolated islets. Uninflated pancreata may result in lack of some important metabolic responses in the isolated islets. Secondly, the loading of the dye/the expression of the sensor defines the signal-to-noise ratio of the time-lapse recording. Signals are absent or attenuated in overloaded islets. Lastly, successful and dense positioning of the tissue inside the imaging chamber is a defining moment for meaningful and analyzable experiments. Poorly positioned or moving tissue results in wasted experimental time and/or unclear data.

The method can be modified to account for multiple signals (using the confocal system) and multiple groups of islets (e.g., of different genotype). Imaging of multiple signals assumes delivery

of a second sensor into each cell of the islet, spectrally compatible with the Ca^{2+} reporter (such as a pH sensor SNARF5f[26,27]). To that end, islets can be co-loaded/co-infected with Ca^{2+} and pH sensors, which are then sequentially imaged within each time-frame.

Imaging the signal in groups of islets with single-cell resolution requires using a wide field-of-view objective. The objective is likely to have lower magnification and numerical aperture (NA), thereby reducing the spatial resolution. Due to the increased depth-of-focus of the low-NA objective, imaging can be performed on a wide-field system. The disadvantages of this arrangement are cell-cell cross-contamination of the light signal and reduced ability to image the 3D signal (e.g., mice expressing the Ca^{2+} sensor under the insulin promoters). At the same time, signal expressed from the surface islet cells can be perfectly resolved with high temporal resolution from groups including tens to hundreds of islets[18].

Although it may sound unpleasant but performing image analysis and numerical data analysis in separate software packages is a good idea. At the current time, ImageJ/FIJI dominates scientific image analysis. The most popular environments for scientific coding are Python and Matlab, yet there are also known efforts to analyze the Ca^{2+} data in R[28]. Best usability is provided by more niche packages like IgorPro. Our choice is to prototype in Matlab/Python and then implement the code in IgorPro for 'pipeline' use. Adapting signal analysis packages for electrophysiology (e.g., Clampfit, Neuroexplorer) for analytical needs can be useful for single-cell imaging but is difficult to scale up. Many options provided by such packages are not applicable for islet imaging because of low sampling rate.

It is important to remember that this methodology is limited by a number of factors. Firstly, as mentioned above, imaging is largely based on undersampling the data, meaning it does not indicate and therefore cannot be directly compared to electrical activity of the cell. Secondly, the data comes from the islet periphery and does not reflect important coupling processes that are, generally speaking, three-dimensional. Thirdly, the level of loading/expression affects the perception of the sensor intensity. Lastly, activation of less well-researched islet cell subpopulations (e.g., PP cells & ϵ-cells) by the marker compounds cannot be ruled out, although due to the low numbers of these cells within the islet any potential contamination will be minimal.

The method is a true 'champion' in terms of visual effect, as the oscillatory processes deliver a strong impression of a genuinely living tissue. Applied to minor cell subpopulations, the method probes the function of each one reliably, allowing identification of subgroups and reflecting the heterogeneity.

Calcium dynamics has been studied in pancreatic islet β-cells for over 40 years, mostly driven by the progress in acquisition/detection technology. Early studies used atomic absorption spectroscopy[29], but it was not until the arrival of fluorescent Ca^{2+} sensors[30] that detailed kinetics could be resolved in individual islet cells, using photometry[31-33]. Soon after that, the spatial component of Ca^{2+} kinetics was improved as Ca^{2+} imaging[34-36] became a routine technology, thanks to the then newly available charge-coupled device (CCD) detectors. The problem of out-

of-focus light, that hampered imaging the signal from individual cells within the tissue, was then resolved in the mid-1990s via laser scanning confocal microscopy (LSCM)[37] and total internal reflection fluorescence microscopy (TIRFM)[38]. Both methods, complemented by the arrival of a new generation of fluorescent Ca^{2+} sensors excitable with a 488 nm laser, have been successfully used to image Ca^{2+} dynamics in the islet cell subpopulations[39-41].

The new century brought forward two new trends that stemmed from neuroscience-related technological developments. Firstly, recombinant fluorescent sensors based on circular permutation of GFP variants substantially increased signal-to-noise ratio for Ca^{2+} detection, effectively bringing the studies to the level of large cell populations, in which the dynamics of $[Ca^{2+}]_{cyt}$ in every cell could be resolved. Secondly, use of tissue-specific promoters allowed targeting sensor expression to minor subpopulations.

Although generally thought to reflect the developments in neuroscience, studies on islet Ca^{2+} dynamics have two key differences. Firstly, technologically, any in vivo imaging of islet signaling is more complex than imaging in the brain due to the unpredictable anatomy of the pancreas and the islets' location[42]. Secondly, excellent electrical coupling between the islet β-cells essentially renders islets into electrically inert populations displaying a seemingly perfect all-or-nothing response to the high glucose stimulus. We believe that studies of $[Ca^{2+}]_i$ kinetics in minor islet subpopulations, such as δ-cells, based on tissue-specific targeting are likely to broaden our knowledge of their pharmacology/physiology. At the same time, highly sensitive probes allow expanding the statistical power of such measurements, accounting to islet-to-islet variability and allowing imaging of islets from different groups within one parallel experiment.

ACKNOWLEDGMENTS:

AH was a recipient of a Diabetes UK PhD Studentship, EV was supported by the OXION-Wellcome Trust Training Programme, AIT held an Oxford Biomedical Research Council postdoctoral fellowship.

DISCLOSURES:

The Authors declare no conflicts of interest.

REFERENCES:

1 Elayat, A.A., el-Naggar, M.M., & Tahir, M. An immunocytochemical and morphometric study of the rat pancreatic islets. *Journal of Anatomy.* **186** (Pt 3), 629 (1995).

2 Cabrera, O. et al. The unique cytoarchitecture of human pancreatic islets has implications for islet cell function. *Proceedings of the National Academy of Sciences of the United States of America.* **103** (7), 2334-2339, doi:10.1073/pnas.0510790103 (2006).

3 Brereton, M.F., Vergari, E., Zhang, Q., Clark, A. Alpha-, delta-and PP-cells: are they the architectural cornerstones of islet structure and co-ordination? *Journal of Histochemistry & Cytochemistry.* **63** (8), 575-591 (2015).

4 Færch, K. et al. Insulin resistance is accompanied by increased fasting glucagon and delayed glucagon suppression in individuals with normal and impaired glucose regulation. *Diabetes.* **65** (11), 3473-3481 (2016).

5 Dabrowski, M., Tarasov, A., Ashcroft, F.M. Mapping the architecture of the ATP-binding site of the KATP channel subunit Kir6. 2. *The Journal ofPhysiology.* **557** (2), 347-354 (2004).
6 Liu, Y.J., Vieira, E., Gylfe, E. A store-operated mechanism determines the activity of the electrically excitable glucagon-secreting pancreatic alpha-cell. *Cell Calcium.* **35** (4), 357-365, doi:10.1016/j.ceca.2003.10.002 (2004).
7 Nakai, J., Ohkura, M., Imoto, K. A high signal-to-noise Ca 2+ probe composed of a single green fluorescent protein. *Nature Biotechnology.* **19** (2), 137 (2001).
8 Nagai, T., Sawano, A., Park, E.S., Miyawaki, A. Circularly permuted green fluorescent proteins engineered to sense Ca2+. *Proceedings of the National Academy of Sciences.* **98** (6), 3197-3202 (2001).
9 Broussard, G.J., Liang, R., Tian, L. Monitoring activity in neural circuits with genetically encoded indicators. *Frontiers in Molecular Neuroscience.* **7**, 97 (2014).
10 Akerboom, J. et al. Optimization of a GCaMP calcium indicator for neural activity imaging. *Journal of Neuroscience.* **32** (40), 13819-13840 (2012).
11 Rodriguez, E.A. et al. The growing and glowing toolbox of fluorescent and photoactive proteins. *Trends in Biochemical Sciences.* **42** (2), 111-129 (2017).
12 Tarasov, A.I. Rutter, G.A. In: *Methods in enzymology.* Vol. **542**, Elsevier, 289-311 (2014).
13 Tarasov, A.I. et al. Frequency-dependent mitochondrial Ca(2+) accumulation regulates ATP synthesis in pancreatic β cells. *Pflugers Archiv: European Journal of Physiology.* **465** (4), 543-554, doi:10.1007/s00424-012-1177-9 (2013).
14 Smith, N.A. et al. Fluorescent Ca2+ indicators directly inhibit the Na, K-ATPase and disrupt cellular functions. *Science Signal.* **11** (515), eaal2039 (2018).
15 Zhao, Y. et al. An expanded palette of genetically encoded Ca2+ indicators. *Science.* **333** (6051), 1888-1891 (2011).
16 Dana, H. et al. Sensitive red protein calcium indicators for imaging neural activity. *Elife.* **5**, e12727 (2016).
17 Theis, L. et al. Benchmarking Spike Rate Inference in Population Calcium Imaging. *Neuron.* **90** (3), 471-482, doi:10.1016/j.neuron.2016.04.014 (2016).
18 Hamilton, A. et al. Adrenaline Stimulates Glucagon Secretion by Tpc2-Dependent Ca(2+) Mobilization From Acidic Stores in Pancreatic alpha-Cells. *Diabetes.* **67** (6), 1128-1139, doi:10.2337/db17-1102 (2018).
19 Adriaenssens, A.E. et al. Transcriptomic profiling of pancreatic alpha, beta and delta cell populations identifies delta cells as a principal target for ghrelin in mouse islets. *Diabetologia.* **59** (10), 2156-2165, doi:10.1007/s00125-016-4033-1 (2016).
20 DiGruccio, M.R. et al. Comprehensive alpha, beta and delta cell transcriptomes reveal that ghrelin selectively activates delta cells and promotes somatostatin release from pancreatic islets. *Molecular Metabolism.* **5** (7), 449-458 (2016).
21 Mourao, M., Satin, L., Schnell, S. Optimal experimental design to estimate statistically significant periods of oscillations in time course data. *PloS One.* **9** (4), e93826, doi:10.1371/journal.pone.0093826 (2014).
22 Zmuda, E.J., Powell, C.A., Hai, T. A method for murine islet isolation and subcapsular kidney transplantation. *Journal of Visualized Experiments.* (50) (2011).
23 Cabrera, O. et al. Glutamate is a positive autocrine signal for glucagon release. *Cell Metabolism.* **7** (6), 545-554, doi:10.1016/j.cmet.2008.03.004 (2008).

24 Thevenaz, P., Ruttimann, U.E., Unser, M. A pyramid approach to subpixel registration based on intensity. *IEEE Transactions on Image Processing.* **7** (1), 27-41 (1998).
25 Tarasov, A.I. et al. Monitoring real-time hormone release kinetics via high-content 3-D imaging of compensatory endocytosis. *Lab on a Chip.* **18** (18), 2838-2848 (2018).
26 Knudsen, J.G. et al. Dysregulation of Glucagon Secretion by Hyperglycemia-Induced Sodium-Dependent Reduction of ATP Production. *Cell Metabolism.* doi:10.1016/j.cmet.2018.10.003 (2018).
27 Adam, J. et al. Fumarate hydratase deletion in pancreatic β cells leads to progressive diabetes. *Cell Reports.* **20** (13), 3135-3148 (2017).
28 Wills, Q.F. et al. Statistical approaches and software for clustering islet cell functional heterogeneity. *Islets.* **8** (2), 48-56, doi:10.1080/19382014.2016.1150664 (2016).
29 Berggren, P.O., Ostenson, C.G., Petersson, B., Hellman, B. Evidence for divergent glucose effects on calcium metabolism in pancreatic beta- and alpha 2-cells. *Endocrinology.* **105** (6), 1463-1468, doi:10.1210/endo-105-6-1463 (1979).
30 Grynkiewicz, G., Poenie, M., Tsien, R.Y. A new generation of Ca2+ indicators with greatly improved fluorescence properties. *The Journal of Biological Chemistry.* **260** (6), 3440-3450 (1985).
31 Longo, E.A. et al. Oscillations in cytosolic free Ca2+, oxygen consumption, and insulin secretion in glucose-stimulated rat pancreatic islets. *The Journal of Biological Chemistry.* **266** (14), 9314-9319 (1991).
32 Johansson, H., Gylfe, E., Hellman, B. Cyclic AMP raises cytoplasmic calcium in pancreatic alpha 2-cells by mobilizing calcium incorporated in response to glucose. *Cell Calcium.* **10** (4), 205-211 (1989).
33 Grapengiesser, E., Gylfe, E., Hellman, B. Three types of cytoplasmic Ca2+ oscillations in stimulated pancreatic β-cells. *Archives of Biochemistry and Biophysics.* **268** (1), 404-407 (1989).
34 Okamoto, Y. et al. Role of cytosolic Ca2+ in impaired sensitivity to glucose of rat pancreatic islets exposed to high glucose in vitro. *Diabetes.* **41** (12), 1555-1561 (1992).
35 Gilon, P. Henquin, J.C. Influence of membrane potential changes on cytoplasmic Ca2+ concentration in an electrically excitable cell, the insulin-secreting pancreatic B-cell. *The Journal of Biological Chemistry.* **267** (29), 20713-20720 (1992).
36 Valdeolmillos, M., Nadal, A., Soria, B., Garcia-Sancho, J. Fluorescence digital image analysis of glucose-induced [Ca2+]i oscillations in mouse pancreatic islets of Langerhans. *Diabetes.* **42** (8), 1210-1214 (1993).
37 Cheng, H., Lederer, W.J., Cannell, M.B. Calcium sparks: elementary events underlying excitation-contraction coupling in heart muscle. *Science.* **262** (5134), 740-744 (1993).
38 Stout, A.L. Axelrod, D. Evanescent field excitation of fluorescence by epi-illumination microscopy. *Applied Optics.* **28** (24), 5237-5242 (1989).
39 Stozer, A., Dolensek, J., Rupnik, M.S. Glucose-stimulated calcium dynamics in islets of Langerhans in acute mouse pancreas tissue slices. *PloS One.* **8** (1), e54638, doi:10.1371/journal.pone.0054638 (2013).
40 Tian, G., Sandler, S., Gylfe, E., Tengholm, A. Glucose- and hormone-induced cAMP oscillations in alpha- and beta-cells within intact pancreatic islets. *Diabetes.* **60** (5), 1535-1543, doi:10.2337/db10-1087 (2011).
41 Benninger, R.K., Zhang, M., Head, W.S., Satin, L.S., Piston, D.W. Gap junction coupling and

749 calcium waves in the pancreatic islet. *Biophysical Journal.* **95** (11), 5048-5061 (2008).
750 42 van Gurp, L. et al. Sequential intravital imaging reveals in vivo dynamics of pancreatic
751 tissue transplanted under the kidney capsule in mice. *Diabetologia.* **59** (11), 2387-2392,
752 doi:10.1007/s00125-016-4049-6 (2016).
753

fig 1

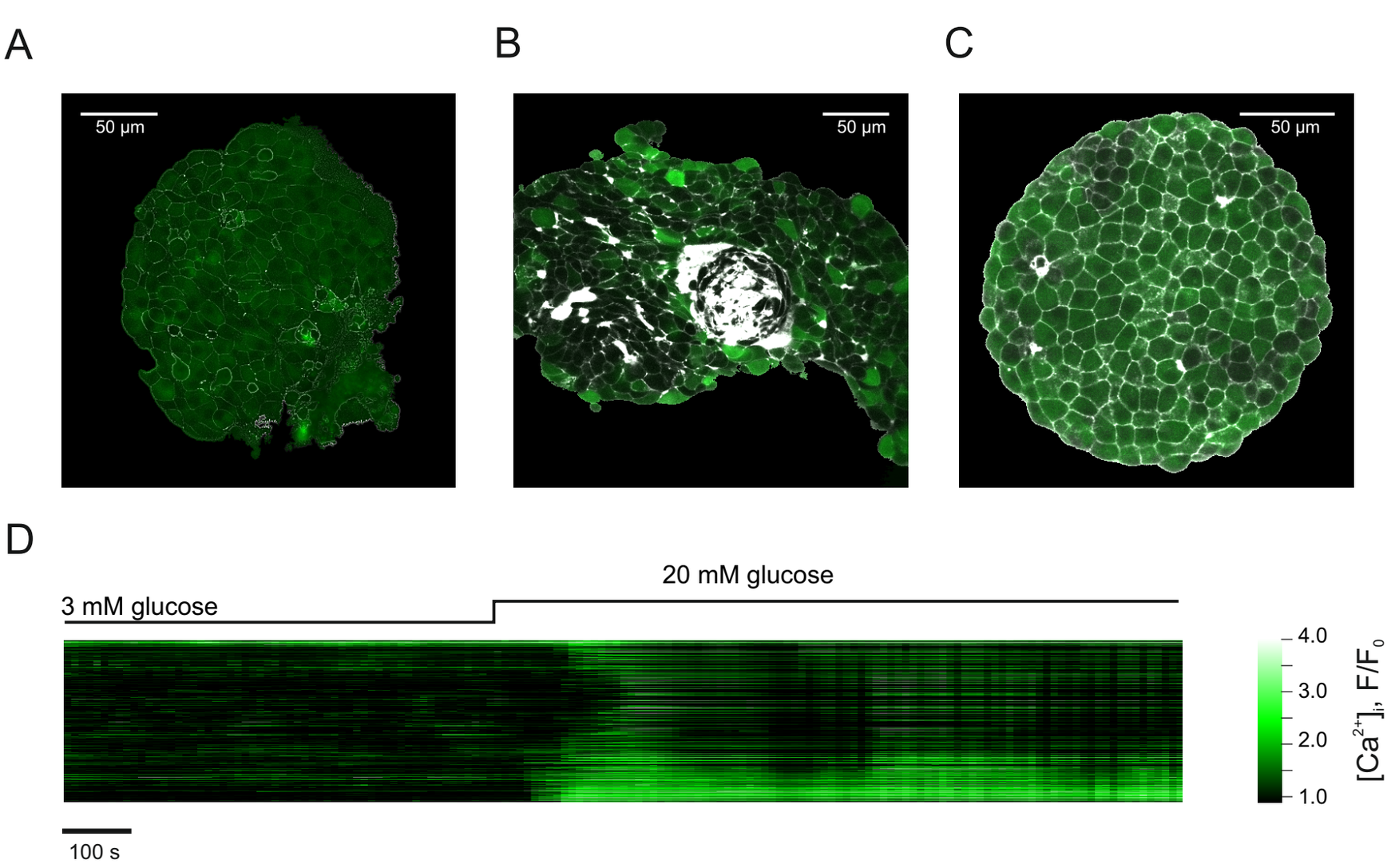

fig 2

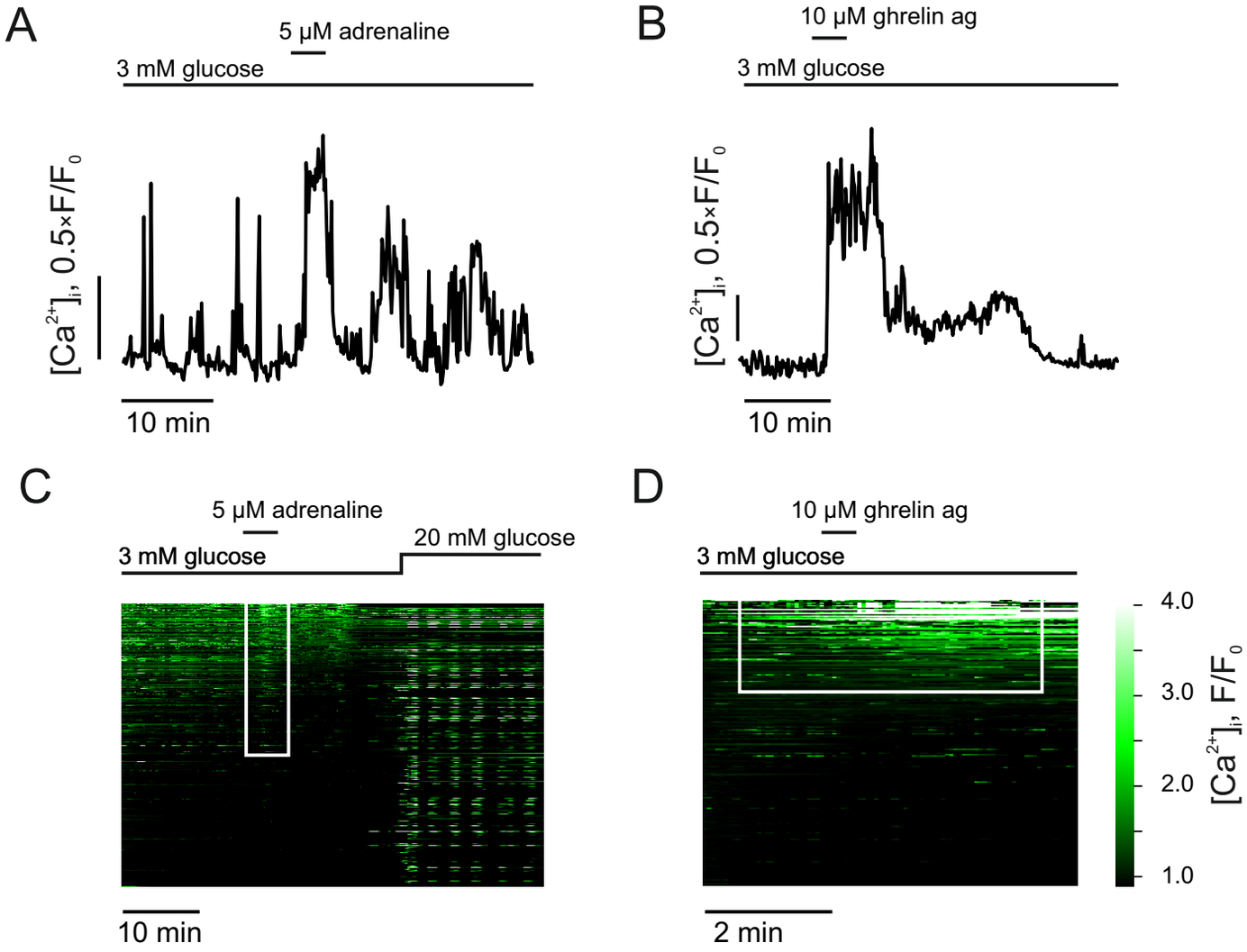
A
5 μM adrenaline
3 mM glucose
[Ca2+]i, 0.5×F/F0
10 min
B
10 μM ghrelin ag
3 mM glucose
[Ca2+]i, 0.5×F/F0
10 min
C
5 μM adrenaline
20 mM glucose
3 mM glucose
10 min
D
10 μM ghrelin ag
3 mM glucose
2 min
4.0
3.0
2.0
1.0
[Ca2+]i, F/F0

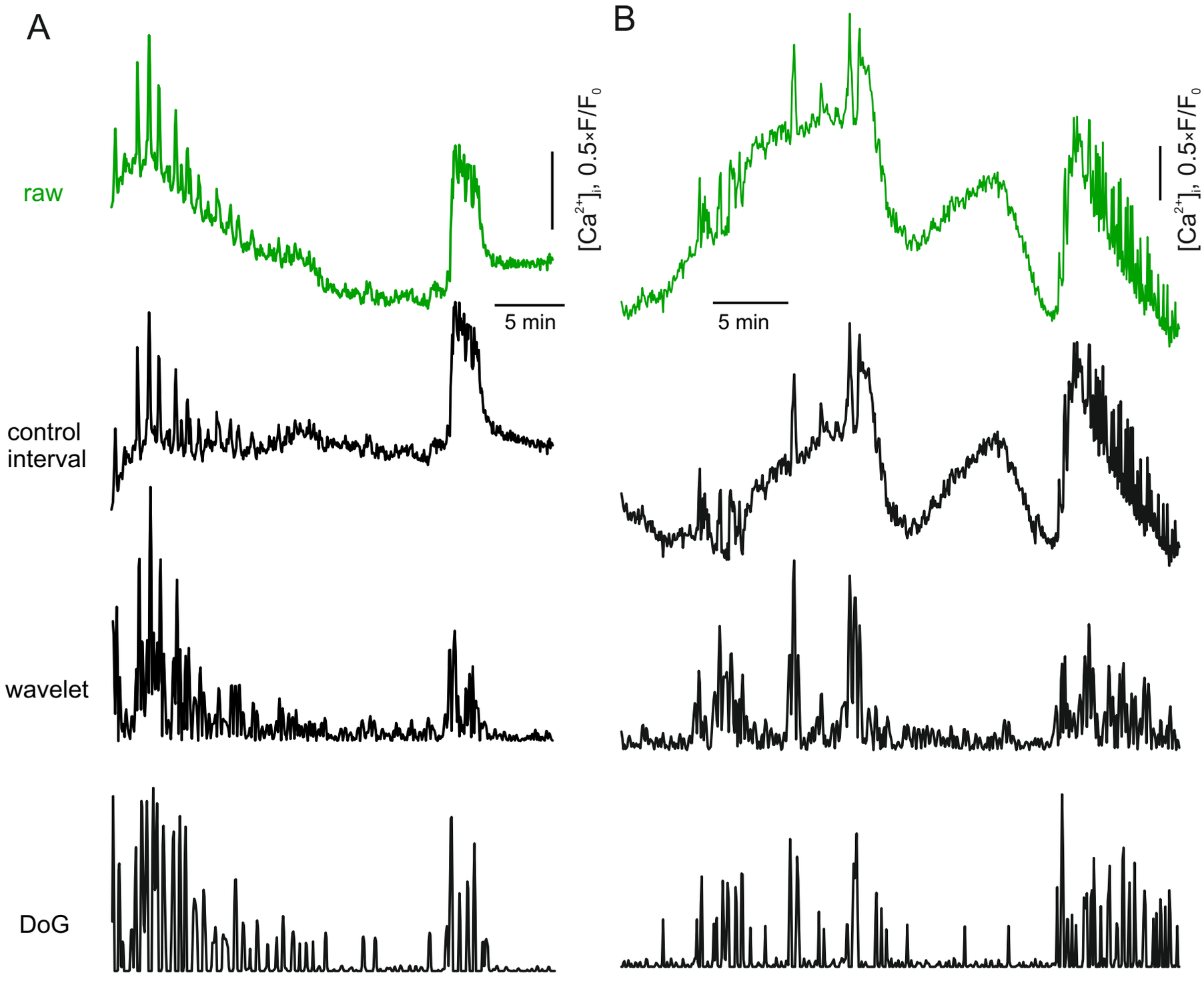
A
B
fig 3
raw
control
interval
wavelet
DoG
5 min
5 min
[Ca2+]i, 0.5×F/F0
[Ca2+]i, 0.5×F/F0

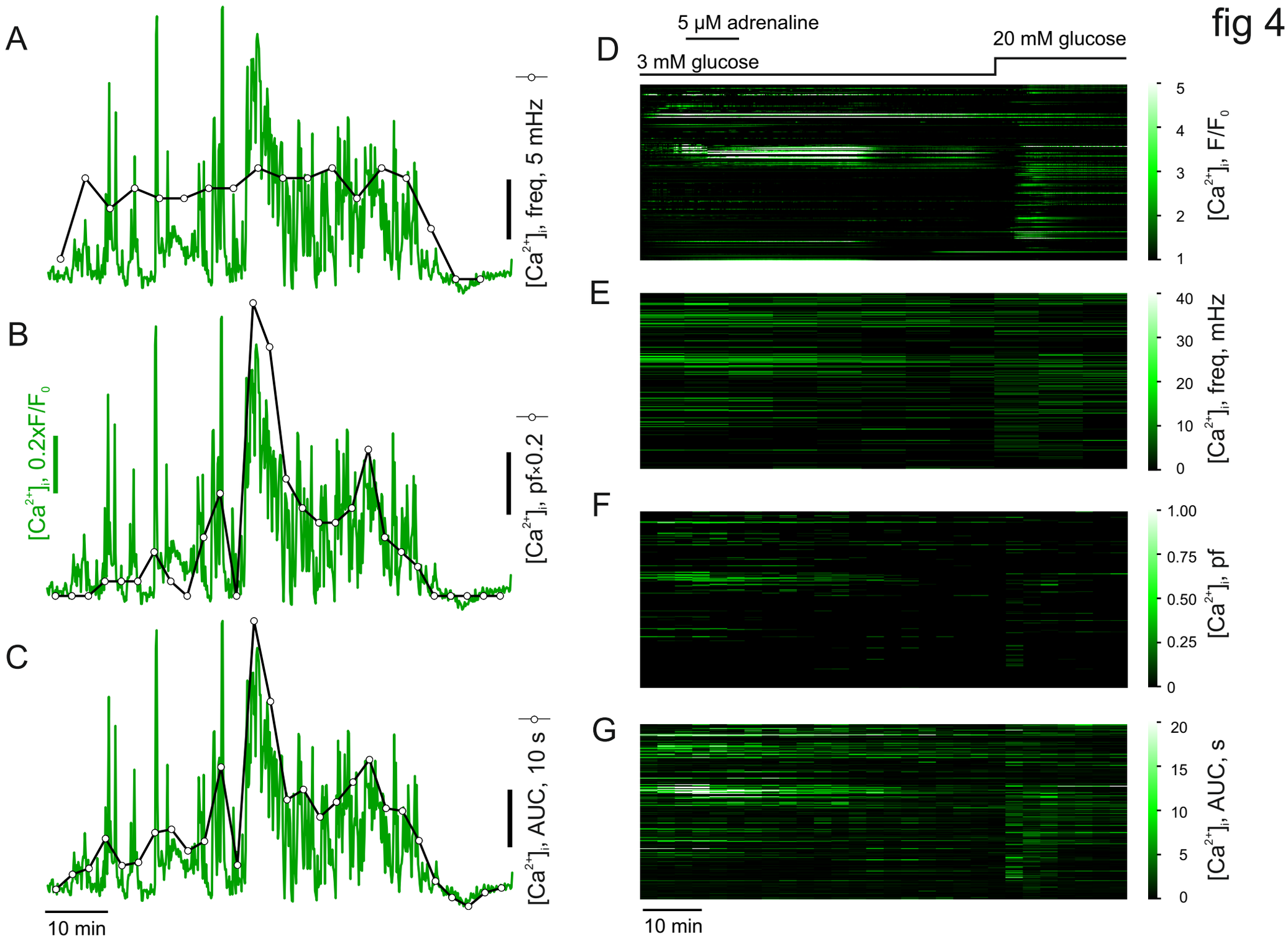
fig 4
A
B
C
D
E
F
G
5 μM adrenaline
3 mM glucose
20 mM glucose
[Ca2+]i, freq, 5 mHz
[Ca2+]i, 0.2xF/F0
[Ca2+]i, pf×0.2
[Ca2+]i, AUC, 10 s
[Ca2+]i, F/F0
[Ca2+]i, freq, mHz
[Ca2+]i, pf
[Ca2+]i, AUC, s
10 min
10 min

Name of Material/ Equipment	Company	Catalog Number	Comments/Description
40x/1.3 objective			
Axiovert 200 microscope			
emission			
Excitation			
Fetal bovine serum	Sigma-Aldrich	F7524-500ML	
Fluo4	ThermoFisher (Life Technologies)	F14201	
GCaMP6f, in (human type 5)			
adenoviral vector	Vector Biolabs	1910	
Hanks' solution	ThermoFisher (GibCo, Life Technologies)		
Liberase	Sigma-Aldrich	5401020001	
penicillin/streptomycin	ThermoFisher (GibCo, Life Technologies)	15140122	
RPMI medium	ThermoFisher (GibCo, Life Technologies)	61870044	
Zeiss LSM510-META confocal			
system	Carl Zeiss		

JOVE JOURNAL OF VISUALIZED EXPERIMENTS
1 Alewife Center #200
Cambridge, MA 02140
tel. 617.945.9051
www.jove.com

ARTICLE AND VIDEO LICENSE AGREEMENT - UK

Title of Article: Imaging calcium dynamics in subpopulations of mouse pancreatic islet cells

Author(s): Alexander Hamilton, Elisa Vergari, Caroline Miranda, Andrei I. Tarasov

Item 1 (check one box): The Author elects to have the Materials be made available (as described at http://www.jove.com/author) via: [X] Standard Access [ ] Open Access

Item 2 (check one box):

[X] The Author is NOT a United States government employee.

[ ] The Author is a United States government employee and the Materials were prepared in the course of his or her duties as a United States government employee.

[ ] The Author is a United States government employee but the Materials were NOT prepared in the course of his or her duties as a United States government employee.

ARTICLE AND VIDEO LICENSE AGREEMENT

1. Defined Terms. As used in this Article and Video License Agreement, the following terms shall have the following meanings: "**Agreement**" means this Article and Video License Agreement; "**Article**" means the article specified on the last page of this Agreement, including any associated materials such as texts, figures, tables, artwork, abstracts, or summaries contained therein; "**Author**" means the author who is a signatory to this Agreement; "**Collective Work**" means a work, such as a periodical issue, anthology or encyclopedia, in which the Materials in their entirety in unmodified form, along with a number of other contributions, constituting separate and independent works in themselves, are assembled into a collective whole; "**CRC License**" means the Creative Commons Attribution 3.0 Agreement (also known as CC-BY), the terms and conditions of which can be found at: http://creativecommons.org/licenses/by/3.0/us/legalcode; "**Derivative Work**" means a work based upon the Materials or upon the Materials and other pre-existing works, such as a translation, musical arrangement, dramatization, fictionalization, motion picture version, sound recording, art reproduction, abridgment, condensation, or any other form in which the Materials may be recast, transformed, or adapted; "**Institution**" means the institution, listed on the last page of this Agreement, by which the Author was employed at the time of the creation of the Materials; "**JoVE**" means MyJove Corporation, a Massachusetts corporation and the publisher of *The Journal of Visualized Experiments;*

"**Materials**" means the Article and / or the Video; "**Parties**" means the Author and JoVE; "**Video**" means any video(s) made by the Author, alone or in conjunction with any other parties, or by JoVE or its affiliates or agents, individually or in collaboration with the Author or any other parties, incorporating all or any portion of the Article, and in which the Author may or may not appear.

2. Background. The Author, who is the author of the Article, in order to ensure the dissemination and protection of the Article, desires to have the JoVE publish the Article and create and transmit videos based on the Article. In furtherance of such goals, the Parties desire to memorialize in this Agreement the respective rights of each Party in and to the Article and the Video.

3. Grant of Rights in Article. In consideration of JoVE agreeing to publish the Article, the Author hereby grants to JoVE, subject to **Sections 4** and **7** below, the exclusive, royalty-free, perpetual (for the full term of copyright in the Article, including any extensions thereto) license (a) to publish, reproduce, distribute, display and store the Article in all forms, formats and media whether now known or hereafter developed (including without limitation in print, digital and electronic form) throughout the world, (b) to translate the Article into other languages, create adaptations, summaries or extracts of the Article or other Derivative Works (including, without limitation, the Video) or Collective Works based on all or any portion of the Article and exercise all of the rights set forth in (a) above in such translations, adaptations, summaries, extracts, Derivative Works or Collective Works and

(c) to license others to do any or all of the above. The foregoing rights may be exercised in all media and formats, whether now known or hereafter devised, and include the right to make such modifications as are technically necessary to exercise the rights in other media and formats. If the "Open Access" box has been checked in **Item 1** above, JoVE and the Author hereby grant to the public all such rights in the Article as provided in, but subject to all limitations and requirements set forth in, the CRC License.

4. Retention of Rights in Article. Notwithstanding the exclusive license granted to JoVE in **Section 3** above, the

Author shall, with respect to the Article, retain the non-exclusive right to use all or part of the Article for the non-commercial purpose of giving lectures, presentations or teaching classes, and to post a copy of the Article on the Institution's website or the Author's personal website, in each case provided that a link to the Article on the JoVE website is provided and notice of JoVE's copyright in the Article is included. All non-copyright intellectual property rights in and to the Article, such as patent rights, shall remain with the Author.

5. Grant of Rights in Video – Standard Access. This **Section 5** applies if the "Standard Access" box has been checked in **Item 1** above or if no box has been checked in **Item 1** above. In consideration of JoVE agreeing to produce, display or otherwise assist with the Video, the Author hereby acknowledges and agrees that, Subject to **Section 7** below, JoVE is and shall be the sole and exclusive owner of all rights of any nature, including, without limitation, all copyrights, in and to the Video. To the extent that, by law, the Author is deemed, now or at any time in the future, to have any rights of any nature in or to the Video, the Author hereby disclaims all such rights and transfers all such rights to JoVE.

6. Grant of Rights in Video – Open Access. This **Section 6** applies only if the "Open Access" box has been checked in **Item 1** above. In consideration of JoVE agreeing to produce, display or otherwise assist with the Video, the Author hereby grants to JoVE, subject to **Section 7** below, the exclusive, royalty-free, perpetual (for the full term of copyright in the Article, including any extensions thereto) license (a) to publish, reproduce, distribute, display and store the Video in all forms, formats and media whether now known or hereafter developed (including without limitation in print, digital and electronic form) throughout the world, (b) to translate the Video into other languages, create adaptations, summaries or extracts of the Video or other Derivative Works or Collective Works based on all or any portion of the Video and exercise all of the rights set forth in (a) above in such translations, adaptations, summaries, extracts, Derivative Works or Collective Works and (c) to license others to do any or all of the above. The foregoing rights may be exercised in all media and formats, whether now known or hereafter devised, and include the right to make such modifications as are technically necessary to exercise the rights in other media and formats.

7. Government Employees. If the Author is a United States government employee and the Article was prepared in the course of his or her duties as a United States government employee, as indicated in **Item 2** above, and any of the licenses or grants granted by the Author hereunder exceed the scope of the 17 U.S.C. 403, then the rights granted hereunder shall be limited to the maximum rights permitted under such statute. In such case, all provisions contained herein that are not in conflict with such statute shall remain in full force and effect, and all provisions contained herein that do so conflict shall be deemed to be amended so as to provide to JoVE the maximum rights permissible within such statute.

8. Likeness, Privacy, Personality. The Author hereby grants JoVE the right to use the Author's name, voice, likeness, picture, photograph, image, biography and performance in any way, commercial or otherwise, in connection with the Materials and the sale, promotion and distribution thereof. The Author hereby waives any and all rights he or she may have, relating to his or her appearance in the Video or otherwise relating to the Materials, under all applicable privacy, likeness, personality or similar laws.

9. Author Warranties. The Author represents and warrants that the Article is original, that it has not been published, that the copyright interest is owned by the Author (or, if more than one author is listed at the beginning of this Agreement, by such authors collectively) and has not been assigned, licensed, or otherwise transferred to any other party. The Author represents and warrants that the author(s) listed at the top of this Agreement are the only authors of the Materials. If more than one author is listed at the top of this Agreement and if any such author has not entered into a separate Article and Video License Agreement with JoVE relating to the Materials, the Author represents and warrants that the Author has been authorized by each of the other such authors to execute this Agreement on his or her behalf and to bind him or her with respect to the terms of this Agreement as if each of them had been a party hereto as an Author. The Author warrants that the use, reproduction, distribution, public or private performance or display, and/or modification of all or any portion of the Materials does not and will not violate, infringe and/or misappropriate the patent, trademark, intellectual property or other rights of any third party. The Author represents and warrants that it has and will continue to comply with all government, institutional and other regulations, including, without limitation all institutional, laboratory, hospital, ethical, human and animal treatment, privacy, and all other rules, regulations, laws, procedures or guidelines, applicable to the Materials, and that all research involving human and animal subjects has been approved by the Author's relevant institutional review board.

10. JoVE Discretion. If the Author requests the assistance of JoVE in producing the Video in the Author's facility, the Author shall ensure that the presence of JoVE employees, agents or independent contractors is in accordance with the relevant regulations of the Author's institution. If more than one author is listed at the beginning of this Agreement, JoVE may, in its sole discretion, elect not take any action with respect to the Article until such time as it has received complete, executed Article and Video License Agreements from each such author. JoVE reserves the right, in its absolute and sole discretion and without giving any reason therefore, to accept or decline any work submitted to JoVE. JoVE and its employees, agents and independent contractors shall have full, unfettered access to the facilities of the Author or of the Author's institution as necessary to make the Video, whether actually published or not. JoVE has sole discretion as to the method of making and publishing the Materials, including,

without limitation, to all decisions regarding editing, lighting, filming, timing of publication, if any, length, quality, content and the like.

11. Indemnification. The Author agrees to indemnify JoVE and/or its successors and assigns from and against any and all claims, costs, and expenses, including attorney's fees, arising out of any breach of any warranty or other representations contained herein. The Author further agrees to indemnify and hold harmless JoVE from and against any and all claims, costs, and expenses, including attorney's fees, resulting from the breach by the Author of any representation or warranty contained herein or from allegations or instances of violation of intellectual property rights, damage to the Author's or the Author's institution's facilities, fraud, libel, defamation, research, equipment, experiments, property damage, personal injury, violations of institutional, laboratory, hospital, ethical, human and animal treatment, privacy or other rules, regulations, laws, procedures or guidelines, liabilities and other losses or damages related in any way to the submission of work to JoVE, making of videos by JoVE, or publication in *JoVE* or elsewhere by JoVE. The Author shall be responsible for, and shall hold JoVE harmless from, damages caused by lack of sterilization, lack of cleanliness or by contamination due to the making of a video by JoVE its employees, agents or independent contractors. All sterilization, cleanliness or decontamination procedures shall be solely the responsibility of the Author and shall be undertaken at the Author's expense. All indemnifications provided herein shall include JoVE's attorney's fees and costs related to said losses or damages. Such indemnification and holding harmless shall include such losses or damages incurred by, or in connection with, acts or omissions of JoVE, its employees, agents or independent contractors.

12. Fees. To cover the cost incurred for publication, JoVE must receive payment before production and publication the Materials. Payment is due in 21 days of invoice. Should the Materials not be published due to an editorial or production decision, these funds will be returned to the Author. Withdrawal by the Author of any submitted Materials after final peer review approval will result in a US$1,200 fee to cover pre-production expenses incurred by JoVE. If payment is not received by the completion of filming, production and publication of the Materials will be suspended until payment is received.

13. Transfer, Governing Law. This Agreement may be assigned by JoVE and shall inure to the benefits of any of JoVE's successors and assignees. This Agreement shall be governed and construed by the internal laws of the Commonwealth of Massachusetts without giving effect to any conflict of law provision thereunder. This Agreement may be executed in counterparts, each of which shall be deemed an original, but all of which together shall be deemed to me one and the same agreement. A signed copy of this Agreement delivered by facsimile, e-mail or other means of electronic transmission shall be deemed to have the same legal effect as delivery of an original signed copy of this Agreement.

A signed copy of this document must be sent with all new submissions. Only one Agreement required per submission.

AUTHOR:

Name:	Andrei Tarasov
Department:	Oxford Centre for Diabetes, Endocrinology and Metabolism
Institution:	University of Oxford
Article Title:	Imaging calcium dynamics in subpopulations of mouse pancreatic islet cells
Signature:	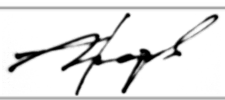
Date:	04 Dec 2018

Please submit a signed and dated copy of this license by one of the following three methods:

1) Upload a scanned copy as a PDF to the *JoVE* submission site upon manuscript submission (preferred);
2) Fax the document to +1.866.381.2236; or
3) Mail the document to *JoVE* / Atn: *JoVE* Editorial / 1 Alewife Center Suite 200 / Cambridge, MA 02140

For questions, please email editorial@jove.com or call +1.617.945.9051.

MS # (internal use):

Replies to the Reviewer's comments

Editorial comments

1. Please take this opportunity to thoroughly proofread the manuscript to ensure that there are no spelling or grammar issues.

Done.

2. As some authors are affiliated with UK institutions, can you please check whether open access is required by your funding agencies?

Checked, no requirement.

3. Keywords: Please provide at least 6 keywords or phrases.

Done

4. Please rephrase the Short Abstract to clearly describe the protocol and its applications in complete sentences between 10-50 words: "Here, we present a protocol to …"

Done.

5. Please revise the Long Abstract to contain no more than 300 words. Please include a statement about the purpose of the method. A more detailed of the method and a summary of its advantages, limitations, and applications is appropriate. Please do not include references here.

Done.

6. Please define all abbreviations before use.

Done.

7. JoVE cannot publish manuscripts containing commercial language. This includes trademark symbols (™), registered symbols (®), and company names before an instrument or reagent. Please remove all commercial language from your manuscript and use generic terms instead. All commercial products should be sufficiently referenced in the Table of Materials and Reagents. You may use the generic term followed by "(see table of materials)" to draw the readers' attention to specific commercial

names. Examples of commercial sounding language in your manuscript are: GibCo, Glutamax, Falcon, Eppendorf, Vector Biolabs, etc.

Done.

8. Please revise the protocol text to avoid the use of any personal pronouns (e.g., "we", "you", "our" etc.).

Done.

9. Please revise the protocol to contain only action items that direct the reader to do something (e.g., “Do this,” “Ensure that,” etc.). The actions should be described in the imperative tense in complete sentences wherever possible. Avoid usage of phrases such as “could be,” “should be,” and “would be” throughout the Protocol. Any text that cannot be written in the imperative tense may be added as a “Note.” Please include all safety procedures and use of hoods, etc. However, notes should be used sparingly and actions should be described in the imperative tense wherever possible. Please move the discussion about the protocol to the Discussion.

Done.

10. 1.2.1: Please specify the age, gender and strain of mouse used.

Done.

11. 1.2.2: Please specify all surgical tools used.

Done.

12. 3.1.4, etc.: Please revise the Protocol steps so that individual steps contain only 2-3 actions per step and a maximum of 4 sentences per step. Use sub-steps as necessary.

Done

13. Section 4: Software steps must be more explicitly explained ('click', 'select', etc.). Please add more specific details (e.g. button clicks for software actions, numerical values for settings, etc.).

For our analysis, we utilize home-written code rather than built-in modules. The detailed steps of the data processing are therefore relevant only to our macros. A compromise solution that we propose is to describe the algorithm that any

researcher would be able to implement using his/her software of choice.

14. Please include single-line spaces between all paragraphs, headings, steps, etc.

We have set the paragraph interval to 12 pt.

15. After you have made all the recommended changes to your protocol (listed above), please highlight 2.75 pages or less of the Protocol (including headings and spacing) that identifies the essential steps of the protocol for the video, i.e., the steps that should be visualized to tell the most cohesive story of the Protocol.

Done, gray highlight.

16. Please highlight complete sentences (not parts of sentences). Please ensure that the highlighted part of the step includes at least one action that is written in imperative tense. Notes cannot usually be filmed and should be excluded from the highlighting. Please do not highlight any steps describing anesthetization and euthanasia.

Done.

17. Please include all relevant details that are required to perform the step in the highlighting. For example: If step 2.5 is highlighted for filming and the details of how to perform the step are given in steps 2.5.1 and 2.5.2, then the sub-steps where the details are provided must be highlighted.

Done.

18. Please upload each Figure individually to your Manager account as a .png, .tiff, .pdf, .svg, .eps, .psd, or .ai file.

Done.

19. Please revise either the figures or their corresponding figure legends so they match. For instance, please add/revise panel labels A-D according to the figure legend of Figure 1.

Done.

20. Please revise the Table of Materials to include the name, company, and catalog number of all relevant supplies, reagents, equipment and software in separate columns in an xls/xlsx file. Please sort the items in alphabetical order according to the name

of material/equipment.

Done

21. References: Please do not abbreviate journal titles.

Done.

Reviewers' comments:

The language in the manuscript is not publication grade. Please employ professional copy-editing services.

Done.

Please note that the reviewers raised some significant concerns regarding your method and your manuscript. Please revise the manuscript to thoroughly address these concerns. Additionally, please describe the changes that have been made or provide explanations if the comment is not addressed in a rebuttal letter. We may send the revised manuscript and the rebuttal letter back to peer review.

Done

Reviewer: 1

Manuscript Summary:
The recording of intracellular free Ca in pancreatic cells is a widely used approach but current users and potential ones should benefit from the experience and insights provided in this manuscript. The authors provide both an overview as well as particulars regarding recording cellular calcium levels of islet subpopulations using wide field or confocal microscopy and include such details as to how to make islets, express sensors, set up appropriate sampling etc.

We thank the Reviewer for his/her kind words.

We are afraid though that the Reviewer may be viewing our mission as detailing the protocols for single-cell Ca2+ imaging. Whilst we fully agree with the majority of his/her points for the single-cell mode, we need to note that our protocol aims at the populational (100-1000… cells) recording. This is the case when the mechanisms are known but the behavior of a certain small subpopulation is an unknown variable. We have rewritten the Introduction to underline this point.

Major Concerns:

1. The authors need to include some better data examples such as recordings showing clean Ca oscillations from mouse islets, comparisons between human and mouse recordings, comparisons between dye and genetically encoded sensors and discuss the limitations presented using probe signals that cannot be converted to absolute free Ca concentrations.

We have now included an explanation on why we focus on recordings with low sampling interval and low signal-to-noise. Although a better recording on a single cell/group of cells is perfectly attainable, scaling the recording up to a population of 100s or 1000s cells always results in a loss of the temporal resolution or the SNR. This effect, known among in the field as the “there is no free lunch in imaging” law is based on the quantal nature of the detectable signal. We reflect this point in the text now, too.

2. No discussion of analysis of oscillation plateau fraction is included, which is a weakness but which will require recordings (as in point 1) that show clear and clean oscillations.

Per classical definition of plateau fraction as the ratio of time spent in the active phase to the total burst period (emanating from early microelectrode recordings of the islet electrical activity[1]): neither α-cells[2], nor δ-cells[3] display the β-cell-like bursting pattern, i.e. there is no plateau in their electrical activity.

Per the plateau fraction in the analytical sense, which we view as an “extension” of the statistical open probability concept used to characterize ion channel kinetics: we have implemented this into our analytical routines now and present the results in Fig 4B,F.

3. No discussion is provided as to how to identify biologically relevant signals vs. noise, as in Fig. 1a.

Thank you for pointing out this omission! Former Fig 1A (current Fig 1A-C) presents loading of the dye (Fig1A) and expression of the recombinant sensor (Fig1B,C). The “noise” present in the images is the second fluorescence channel, polar tracer SRB, which we used to outline cells within the islet. We explain this point now, in the figure legend.

4. While it is appreciated that an inherent difficulty with an article of this type is the wide variety of approaches and equipment out there in use, some details about sampling rates, Nyqvist Criteria, binning, choice of best objectives to use, and statistics might help especially new users.

We spell out now that the Nyquist criteria discussion is not applicable in our case (all the recordings are inevitably substantially undersampled as we are dealing with large field-of view experiments). We added more details on objectives too, although we state that the goal can be achieved by a range of optics.

5. The authors' opinion that AUC is best to report is their opinion; this measurement lumps changes in amplitude with frequency and has limitations regarding underlying mechanism. I also doubt that measuring spike frequency is the best one can do to represent data; they should show examples to prove that.

We agree with the Reviewer regarding the limitations of the pAUC: it is (by definition) unable to differentiate between different mechanisms of Ca2+ elevation. However, for effect with known mechanism but unknown populational picture (such as Ca2+ dynamics in 100s of islet cells), pAUC proved to be most robust. That is, a metric that allowed reliable comparison between different recordings without a substantial recording-to-recording variation in the basal/control values.

We have to politely note that we believe AUC to be a fairly confusing characteristic, which is frequently used on a liberal time interval, in biomedical research. We therefore suggest to use this metric on a per-time basis, i.e. as a partial or interval area under the curve.

6. More details are sorely lacking in the figure Legends, especially regarding the images shown and the heat maps.

Thank you for pointing this out, the figure legends have been revised.

7. The paper has many errors of English usage and odd phrasing here and there and will require thorough re-editing.

Done.

Reviewer: 2

The manuscript discusses islet isolation, and calcium imaging with a focus on the minor cell populations that secrete glucagon and somatostatin rather than insulin. It describes chemical dye, and protein based imaging strategies with subsequent image analysis. In general it is understandable, and a fair reflection of how to do this technique, but there are times when syntax is confusing, or articles (the/an) are used incorrectly or omitted where they should be present. These should be possible to fix at copy-editing.

We thank the Reviewer and apologize for omission of the articles. Personally, we do not see much point in using them but welcome JoVE to correct this misconception of ours at the copy-editing stage.

Major Concerns:
1. Dyes such as Fluo4 have significant toxicities (Smith NA, Kress BT, Lu Y, Chandler-Militello D, Benraiss A, Nedergaard M. Fluorescent Ca(2+) indicators directly inhibit the Na,K-ATPase and disrupt cellular functions. Sci Signal. 2018;11(515). Epub 2018/02/01. doi: 10.1126/scisignal.aal2039. PubMed PMID: 29382785.) some of these will be relevant to the islet, this should be discussed.

Thank you. We cite/discuss the paper now. Overall, we believe the effects presented by Smith NA et al could result from overloading and other 'collateral damage' that loading can do (such as interaction of pluronic acid with cell membrane). Having measured the membrane potential using perforated-patch alongside imaging cytosolic [Ca2+] using Fura-Red[4], we doubt that the effects reported by Smith NA et al are significant in our system.

2. The reason why GECI's cannot be imaged rapidly is not explained - protein expression (related to viral infection) and chromophore maturation are both limiting factors. A general overview of FP's/GECI's might be helpful to include as most published literature uses chemical dyes suggesting this tool set is not widely known among islet biologists, a broad reference eg DOI: 10.1016/j.tibs.2016.09.010, might be worth including. If there are consequences for islet biology due to "de-differentiation" in culture over this time period these issues should be discussed.

We thank the Reviewer for this reference which has now been cited in the text. We have been actively using GECI as well as recombinant sensors for other analytes for over 10 years by now (the outputs having been published since 2012 – pubmed Tarasov AI[au]) and do our very best to popularize this toolset within

the ‘islet’ community.

3. The claims made about red GECI's (line 103-105) not working in tissue imaging because of low SNR seems difficult to reconcile with their imaging characteristics (red light is better for this than green light). The authors suggest single cell data is good, and the only example I could find (Chang YF; Broyles CN, Brook FA; Davies MJ; Turtle CW; Nagai T & Daniels MJ. Non-invasive phenotyping and drug testing in single cardiomyocytes or beta-cells by calcium imaging and optogenetics. PLOSone, 2017, 12, e0174181.) certainly appears to support that view. As far as I know there is no comparative SNR study on the utility of the GECI's in single cells or islets.

As dyes appear hazardous (point 1), and proteins offer an under-utilitzed alternative (point 2) I think it would advantage this manuscript if a simple table catalogued the GECI, the cell type/islet, publication reference, and commercial supplier (if relevant) used in this field.

Thank you, we accept this correction and have rewritten the Introduction accordingly.

We have to politely decline the request for presenting the catalogue of successful uses of recombinant sensors with islet cells as we believe this goes beyond the scope of our *de facto* protocol paper. We prefer focusing on our findings/developments.

4 Would it be possible to show "Before" and "After" examples of successful (and unsuccessful) baseline corrections. This is very challenging for novices to understand, and because of the fluctuation in signal due to calcium itself can be difficult to do. Islet samples from humans are precious so every effort must be made not to discard data, but sometimes it is impossible to adequately correct for bleaching/sample drift and including examples that can't be analyzed would be helpful I believe. In particular baseline corrections that produce drifts up, or continued drifts down should be shown. As the authors point out, peak counts may still be possible in these samples, but AUC analyses might not be.

Thank you for the suggestion. We are providing the examples of baseline correction now (Fig 3).

Having screened human islet performance from around 100 donors within last 7 years, we have to politely disagree with the Reviewer’s point regarding inclusion of as many samples as possible, from human material. In ‘real world’, the main

impact on the experimental performance of human islet preparation (in terms of glucose sensing) is made by the isolation procedure, which is understandably complex/prolonged in this case. Every well-isolated human sample is indeed very precious – but samples like that are just as good as their mouse counterparts, i.e. do not require any special effort in terms of data extraction, please see examples[5,6]. Despite being very much capable of extracting/counting peaks from essentially any sample, independently of bleaching (as shown in Fig 3), we naturally oppose any manipulation that may generate artefacts. We regard any published work on human tissue that fails to present high-quality raw data as potential fraud and have added a cautionary statement in the Discussion now.

5 Some effort is made to discuss alternative wide-field or confocal imaging approaches but the main point I feel is missed, and the resulting message is confused.

Widefield imaging with deconvolution is better than confocal imaging for thin, dim samples. In this case there is sample thickness and confocal detectors are therefore preferable. However confocal line scanning illumination is relatively high power (causing photobleaching, and phototoxicity), slow, and historically offers much lower detector sensitivity than the widefield equivalents. It is probably beyond the scope of this article to go into the solutions to these problems, but suffice it to say that they can be overcome by different equipment configurations.
I would try and steer away from what at times is quite a poorly constructed discussion about the two approaches and keep this simple and describe in a little more detail the imaging apparatus used in this study (as a minimum this should be microscope stage (supplier, model), light source - (type, wavelength and power density at the sample), objective lens (supplier, magnification, numerical aperture) - filters (excitation, dichroic and emission filters), and detector apparatus (make, model, QE for the emission used, frame rate, imaging duration), so that people know what technical requirements are needed if they try to do this. Of course it will always be possible to go bigger, better, faster, and more, but describing a "minimum specification" might be helpful.
The discussion lines 445-456 is a sufficient overview of various imaging technologies that might be acquired by aficionados, but I suspect that these will not be the principle readers of this article, so I would adopt a more simple, didactic approach based on what was used by the authors.

We have to point out that we are not talking about high NA wide-imaging and deconvolution. The choice is between high-NA confocal (that provides superior

spatial resolution but smaller field of view) and low-NA wide-field (that has much larger field-of-view and in principle does not require any deconvolution, as the depth of focus is much larger, which attenuates the cross-contamination). In our hands, the confocal with NA>0.75 is perhaps more sensitive than the wide-field AxioZoom.V16 (NA=0.57, zoom factor=6) but the latter provides a 100x larger field-of view. We do not believe there is much point in using high NA wide-field for tissue imaging as the deconvolution option is not going to help here.

We agree with the main points regarding the comparison of confocal vs wide-field imaging options – perhaps apart from exceptional phototoxicity/photobleaching of the confocal mode. We have re-written the discussion to reflect the point above and added the specification of the imaging systems into the materials worksheet.

Minor Concerns:
6. Nomenclature - GCaMP not GCamp, Ca2+ not always superscripted 2+,

Corrected, thank you.

7. Collagenase or Liberase - is there a preferred supplier or batch?

We agree that batch-to-batch activity variation *may* become a critical issue when islets from older animals (including human donors) are isolated. This is less the case for <26 week old mice, which are used in our work. We therefore provide an optional advice to test the reagent activity and refer to a protocol focused on islet isolation[7].

We have deleted all the references to collagenase: although we have an experience of using it, mentioning two enzymes complicates the protocol.

8 How to aspirate the isolation solution - this is not described (line 153)

Thank you, added “Aspirate gently, with a 10 mL serological pipette.”

9 Is the RPMI supplied with Phenol Red? - Phenol red free alternatives are available that improve the ability to see red signals

Yes, RPMI has Phenol Red and this is a correct point for routine monitoring of the cultured tissue. We do not use RPMI as an imaging solution though; our imaging solution is indicator-free.

10 What is "imaging solution" this is not defined - 2.3.1 (line 179)

Thank you, added now.

11 standard abbreviation for numerical apperture is NA not n.a. (line 248)

Corrected, thank you.

12 dye loading - "overloading" examples might be helpful for the novice (section 2.4.5)

13 viral transduction - unacceptable cell morphology examples (line 208) may help the novice.

We provide a description of the typical signs that could indicate problems.

14 Perfusion (not perifusion) throughout.

We do distinguish between the two terms above and believe that true ‘perfusion’ is achieved when blood capillary system is used (such as in pancreas perfusion technique). To avoid confusion, we use ‘perifusion’ whenever the solution is supplied just outside of the islet and not forced/or facilitated through. We do agree though that the solution does go through the islet in this case, too, but this happens via diffusion. We suggest to leave as is and omit the reasoning above from the text, for the sake of brevity.

Reviewer: 3

Manuscript Summary: This is a nice paper from a strong group of scientists that will be helpful to islet physiologists. I was unable to see the accompanying video to judge it.

Thank you. As far as we are aware the protocol video has not been produced yet but propose the videos of Ca^{2+} dynamics instead, as a “starter” (may not playback in the browser but can be downloaded).

Mouse islet , fluo-4:
https://www.dropbox.com/s/77dzss8zehd5ig4/mouse_islet_fluo4.gif?dl=0

Mouse islet, GCaMP3:
https://www.dropbox.com/s/96kwqag4lwraxjy/Ca_oscillations_mouse_islet.gif?dl=0

References

1 Meissner, H. & Schmelz, H. Membrane potential of beta-cells in pancreatic islets. *Pflügers Archiv.* **351** (3), 195-206 (1974).

2 Zhang, Q. *et al.* Role of KATP channels in glucose-regulated glucagon secretion and impaired counterregulation in type 2 diabetes. *Cell metabolism.* **18** (6), 871-882, doi:10.1016/j.cmet.2013.10.014 (2013).

3 Zhang, Q. *et al.* R-type Ca(2+)-channel-evoked CICR regulates glucose-induced somatostatin secretion. *Nat Cell Biol.* **9** (4), 453-460, doi:10.1038/ncb1563 (2007).

4 Tarasov, A.I. *et al.* Frequency-dependent mitochondrial Ca(2+) accumulation regulates ATP synthesis in pancreatic β cells. *Pflugers Archiv : European journal of physiology.* **465** (4), 543-554, doi:10.1007/s00424-012-1177-9 (2013).

5 Wills, Q.F. *et al.* Statistical approaches and software for clustering islet cell functional heterogeneity. *Islets.* **8** (2), 48-56, doi:10.1080/19382014.2016.1150664 (2016).

6 Tarasov, A.I. *et al.* Monitoring real-time hormone release kinetics via high-content 3-D imaging of compensatory endocytosis. *Lab on a Chip.* **18** (18), 2838-2848 (2018).

7 Zmuda, E.J., Powell, C.A., & Hai, T. A method for murine islet isolation and subcapsular kidney transplantation. *Journal of visualized experiments: JoVE.* (50) (2011).